# Chapter 7

# Experimental Validation of the Finite Element Model and Investigation into Factors Causing the Observed Power Loss

## *7.1* Introduction

The detailed optical and heat transfer analysis of an ACPPVC was reported in chapters 2 and 4. Chapters 5 and 6 detailed the indoor and outdoor experimental analysis undertaken of three trough and five trough ACPPVC-50 systems and a similar non-concentrating flat panel. From this it was observed that under realistic conditions the concentrating PV panel achieved a concentration of approximately 1.65 instead of the theoretical value of 2.0. The detailed optical and heat transfer analysis was undertaken using a modified version of the comprehensive unified model (Eames et al., 2001) suited to solar photovoltaic applications. The model has been verified in this instance by determining the temperature at several locations on the aluminium back plate and the reflector troughs along with the I-V curve of the ACPPVC-50 system.

## *7.2* FE Model and Experimental Investigation of the ACPPVC-50 System

An In-house developed finite element based modified version of comprehensive unified model (Eames et al., 2001) has been used for the analysis of the optics and heat transfer in single trough, triple and five-trough ACPPVC-50's. The model was validated using the experimental data presented in Chapter 6.

### *7.2.1* The External Conditions Applied for Experimental Characterisation of the ACPPVC-50 System

The experiments were conducted outside for a wide range of PV string connections and climatic conditions ranging over a 10-12 hour period.

#### *7.2.1.1* Solar Radiation Intensity Measurement

Two Kipp & Zonen pyranometers were used to measure the intensity of solar radiation incident at the aperture cover of the ACPPVC-50 system. Both pyranometers were placed either side of the experimental test system as shown in figure 6.4.6.1 (see page 211). Both pyranometers showed less then 1% variation of solar radiation intensity when measured throughout individual measurement sweep periods. The average solar radiation intensity values between the two pyranometers were considered for each individual I-V curve and thus validating the finite element model.

#### *7.2.1.2* Ambient Temperature Measurements

The ambient environmental temperature was measured using T-type thermocouples and was found to vary between 15°C to 24°C during the test periods. An ambient temperature of 20°C was considered for validating the model. Wind speed and external weather conditions will effect the temperature measurements, each temperature was measured three times and averaged though the high speed data acquisition system. The accuracy of the thermocouple measurements was ±0.1°C, equivalent to approximately 0.5% of the readings.

#### *7.2.1.3* Wind Speed Measurement

The wind speed was measured at the top of the experimental test system by using an hot wire anemometer and averaged. The minimum and maximum wind speeds were measured at 0.2 $ms^{-1}$ and 5.0 $ms^{-1}$ respectively. A 5% variation from this value can be expected at the aperture cover glass as the wind velocity at the aperture cover and at the aluminium back plate changes the rate of convective heat transfer and thus surface temperatures.

### *7.2.2* The Convective Heat Loss Coefficient Used for Validation of the ACPPVC-50 Finite Element Model

A heat transfer coefficient of 12 $Wm^{-2}K^{-1}$ was considered at the aperture glass cover based on a wind speed of 2 to 3 $ms^{-1}$ (page 101). The heat loss from the back of the aluminium back plate was considered as a flat plate surface of temperature $T_s$ = 60ºC and an ambient temperature of 20ºC. The properties of air were considered at the mean temperature of 40ºC.

The dimensionless numbers used in these calculations were (Incropera and DeWitt, 1996):

$$\text{Reynolds number: } \mathrm{Re} = \frac{uL}{\upsilon}$$

$$\text{Prandtl number: } \mathrm{Pr} = 0.668$$

where u is the air velocity, L is the characteristic dimension i.e. the length of the aluminium back plate and $\upsilon$ is the kinematic viscosity ($1.72\times10^{-5}$ $m^2s^{-1}$ at a temperature of 40ºC). The minimum and maximum wind speeds measured on a day were 0.5 $ms^{-1}$ and 5 $ms^{-1}$.

The Reynolds numbers for these values are

$$\mathrm{Re}_{\min} = \frac{0.5ms^{-1}\times 0.535m}{1.79\times10^{-5}m^2s^{-1}} = 14944$$

and

$$\mathrm{Re}_{\max} = \frac{5.0ms^{-1}\times 0.535m}{1.79\times10^{-5}m^2s^{-1}} = 149441$$

One can therefore assume that the convective flow at the rear of the aluminium back plate is laminar or turbulent (Incropera and DeWitt, 1996) and the following co-relations used to calculate the heat loss coefficient.

$$Nu = \frac{h_{c,\min} L}{k} \equiv 0.664 \times (\mathrm{Re})^{\frac{1}{2}} (\mathrm{Pr})^{\frac{1}{3}} \text{ For laminar flow} \tag{7.2.2.1}$$

$$Nu = \frac{h_{c,\max} L}{k} \equiv 0.037 \times (\mathrm{Re})^{\frac{4}{5}} (\mathrm{Pr})^{\frac{1}{3}} \text{ For turbulent flow} \tag{7.2.2.2}$$

From equations (7.2.2.1) and (7.2.2.2) the minimum and maximum heat loss coefficients are

$$\begin{aligned} h_{c,\min} &= 3.706 \quad Wm^{-2}K^{-1} \\ &and \\ h_{c,\max} &= 23.29 \quad Wm^{-2}K^{-1} \end{aligned} \tag{7.2.2.3}$$

An average heat loss coefficient at the rear of the aluminium back plate 13.5 $Wm^{-2}K^{-1}$ was used to validate the finite element model.

## *7.3* Parametric Analysis to Determine the Effect of Different Heat Transfer Coefficient on the Behaviour of an ACPPVC-50 System

Using the model developed for optics and heat transfer in asymmetric compound parabolic photovoltaic concentrators, simulations were undertaken for different heat loss coefficients at the rear aluminium back plate. Other boundary conditions were used as specified in chapter 4. The three heat loss coefficients used in the simulations were

- a minimum of 3.7 $Wm^{-2}K^{-1}$ (corresponding to a minimum wind speed of 0.5 $ms^{-1}$)
- an average heat loss coefficient of 13.5 $Wm^{-2}K^{-1}$
- a maximum heat loss coefficient of 23.3 $Wm^{-2}K^{-1}$ (corresponding to a maximum wind speed of 5.0 $ms^{-1}$).

Figure 7.3.1 shows the theoretically predicted isotherms of the ACPPVC-50 for the three different heat loss coefficients at the rear aluminium back plate. The isotherms are at 1°C intervals and the solar radiation was 900 $Wm^{-2}$ incident at an angel of 60° at the aperture cover. The maximum predicted temperature at the solar cell was 99°C for a heat loss coefficient of 3.7 $Wm^{-2}K^{-1}$ from the rear aluminium back plate i.e. for very low wind speed of 0.5$ms^{-1}$. Because of the increased convective flow and turbulence for a wind speed of 5$ms^{-1}$ at the rear aluminium back plate, the maximum predicted solar cell temperature is 41°C using a heat loss coefficient from the rear aluminium back plate of 23.3 $Wm^{-2}K^{-1}$. As expected the thermal plumes are thinner and longer as the heat loss coefficient reduces but for all heat loss coefficients the minimum and maximum temperature gradient is adjacent to the solar cell and adjacent to the aperture cover.

Figure 7.3.2 shows an enlarged view of the predicted isotherms and velocity vectors for the ACPPVC-50 when the heat loss coefficient at the rear aluminium plate was 3.7 $Wm^{-2}$ $K^{-1}$ for the 1st and

5th troughs. The velocity vectors are scaled to the reference vector of magnitude 0.2 $ms^{-1}$. The magnitude of the velocity vectors are small inside a large part of the cavity compared to near the boundary. The central region of the concentrator developed few secondary circulations for both individual reflector troughs however in all conditions the velocity vectors are very small in the space between consecutive reflector troughs. This is due to the temperature gradient across the metal boundary being very small. An average temperature difference of 60°C occurred between the aperture cover and the solar cell surface.

Figure 7.3.3 shows an enlarged view of the isotherms and velocity vectors in the 2nd and 4th reflector troughs when the heat loss coefficient from the real aluminium plate is 13.5 $Wm^{-2} K^{-1}$. The enlarged view of the isotherms and velocity vectors of the 1st and 5th troughs of the ACPPVC-50 are shown in figure 7.3.4 at a heat loss coefficient of 23.3 $Wm^{-2}K^{-1}$ from the rear aluminium back plate. The velocity vectors are scaled to the reference vector of magnitude of 0.2 $ms^{-1}$. The thermal plumes are thicker, however the basic distribution of the isotherms remains similar for all simulations. The maximum predicted temperature rise at the solar cell surface is 54°C, the average temperature difference between the aperture cover and the solar cell surface is 25°C. This temperature difference is reduced to 12°C when the heat loss coefficient from the aluminium back plate is 23.3 $Wm^{-2}K^{-1}$ as shown in figure 7.3.4 (a). A significant reduction of the solar cell surface temperature results due to the high wind speed leading to increased convective heat transfer from the rear of the aluminium back plate.

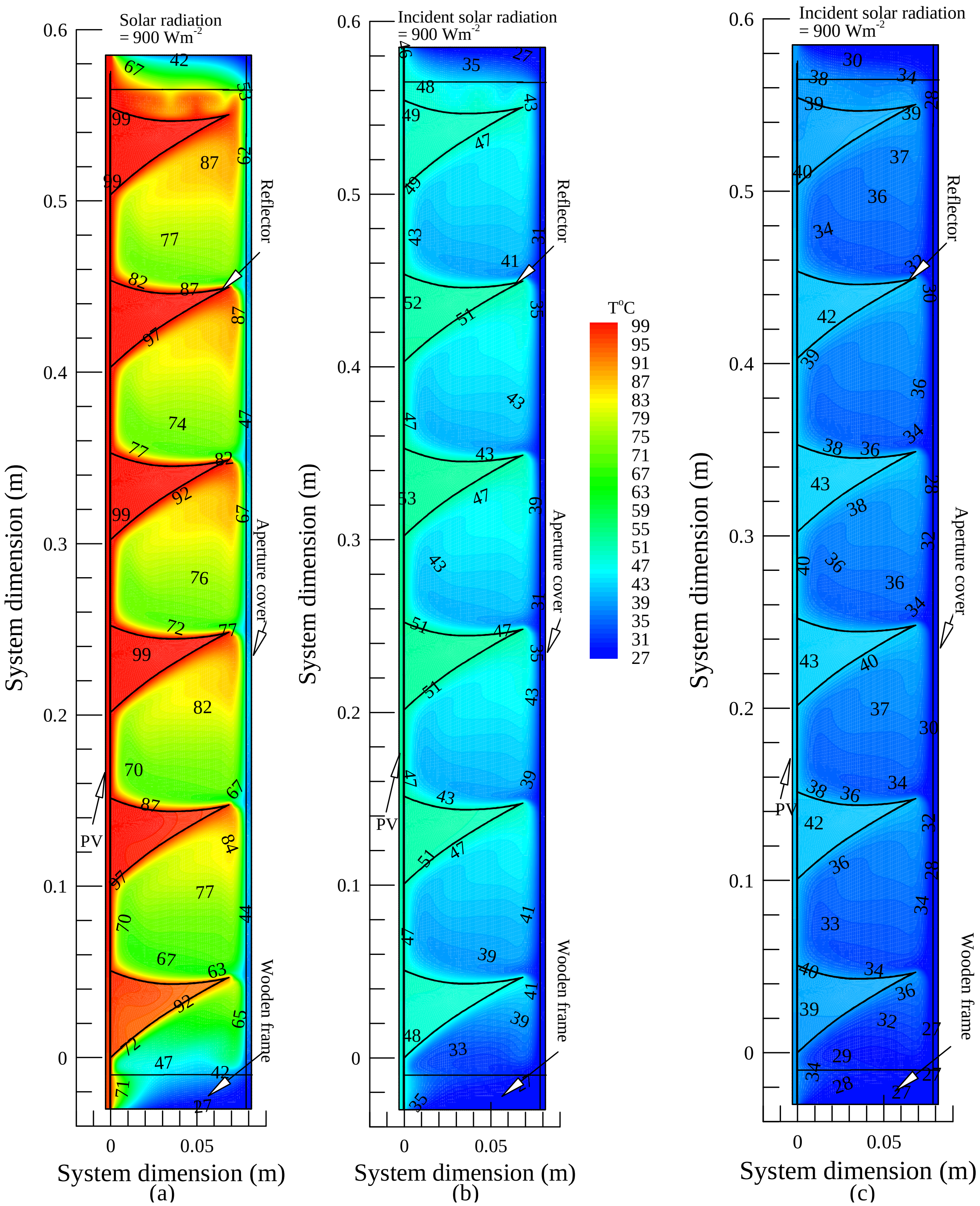


Figure 7.3.1 The theoretically predicted isotherms for an ACPPVC-50 with heat loss from the aluminium back plate of (a) 3.7 $Wm^{-2}K^{-1}$, (b) 13.5 $Wm^{-2}K^{-1}$ and (c) 23.3 $Wm^{-2}K^{-1}$. The isotherms are at 1°C intervals. The solar radiation intensity was 900 $Wm^{-2}$ incident at the aperture cover at an angle of 60°.

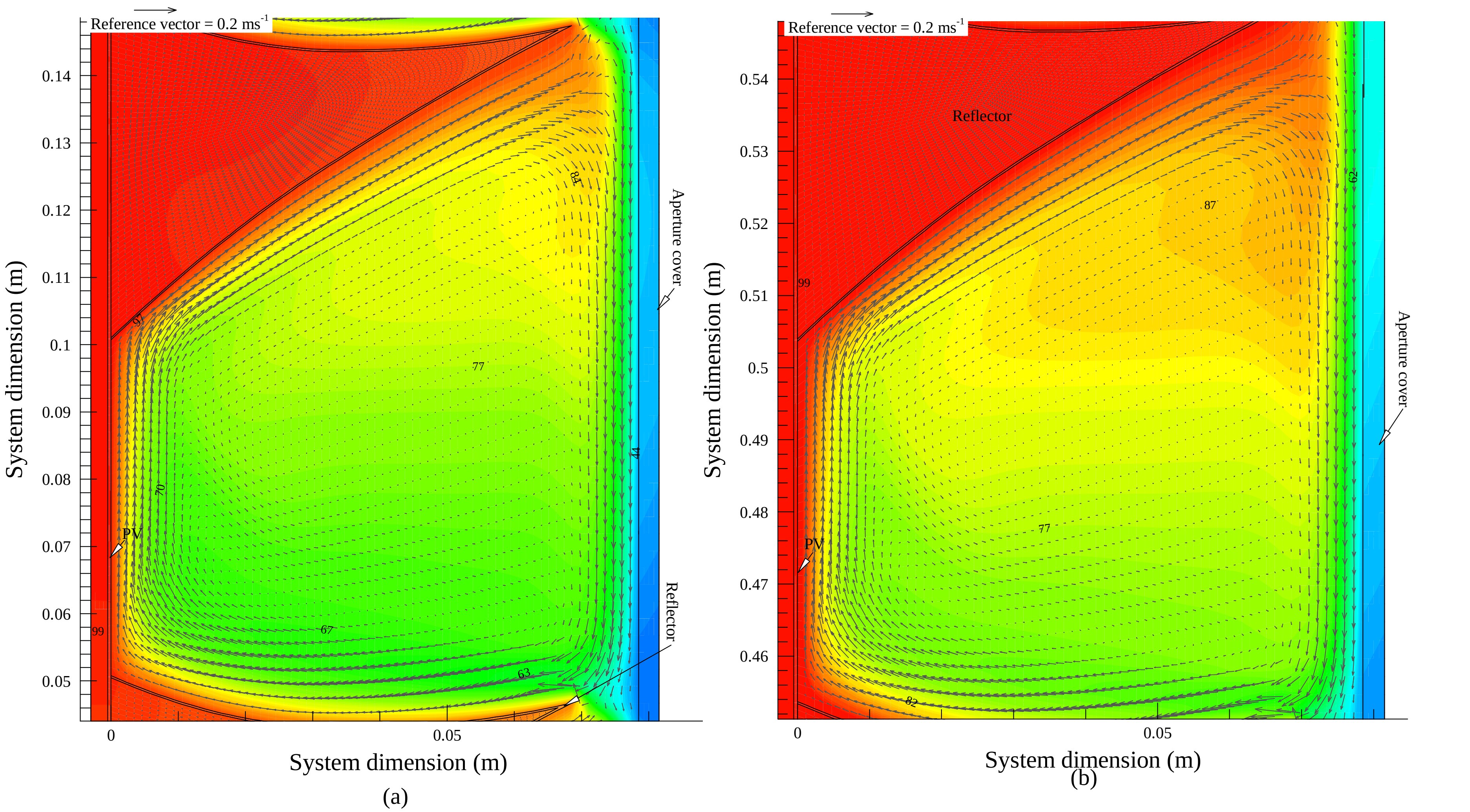


Figure 7.3.2 The enlarged view of predicted isotherms and velocity vectors of ACPPVC-50 with heat loss from the aluminium back plate of 3.7 $Wm^{-2}K^{-1}$ inside (a) 1st trough (b) 5th trough. The isotherms are at 1°C intervals. The velocity vector is scaled to the reference vector of magnitude 0.2 $ms^{-1}$. The solar radiation intensity was 900 $Wm^{-2}$ incident at the aperture cover at an angle of 60°.

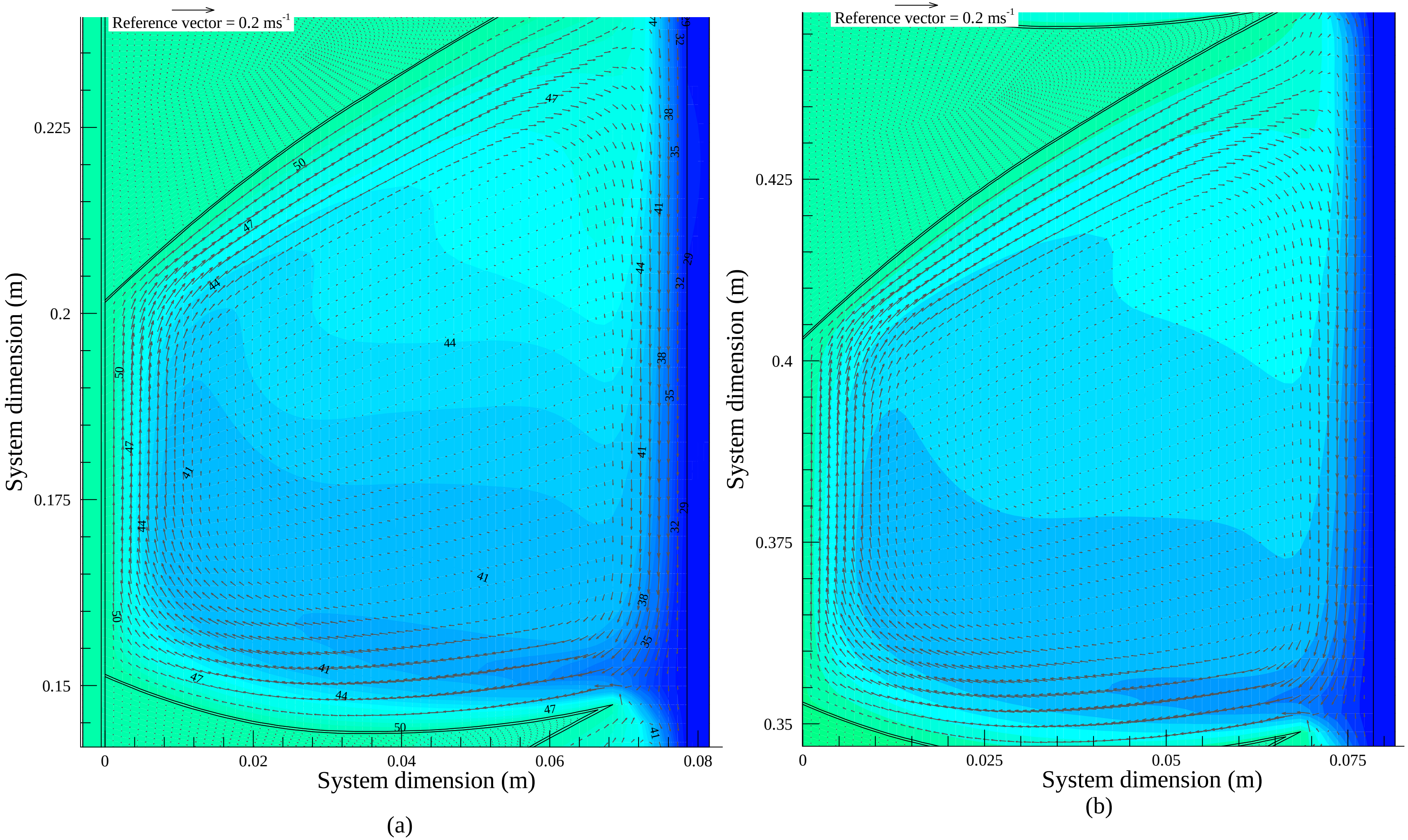


Figure 7.3.3 The enlarged view of predicted isotherms and velocity vectors of ACPPVC-50 with heat loss from the aluminium back plate of 13.5 $Wm^{-2}K^{-1}$ inside (a) 2nd trough (b) 4th trough. The isotherms are at 1°C intervals. The velocity vector is scaled to the reference vector of magnitude 0.2 $ms^{-1}$. The solar radiation intensity was 900 $Wm^{-2}$ incident at the aperture cover at an angle of 60°.

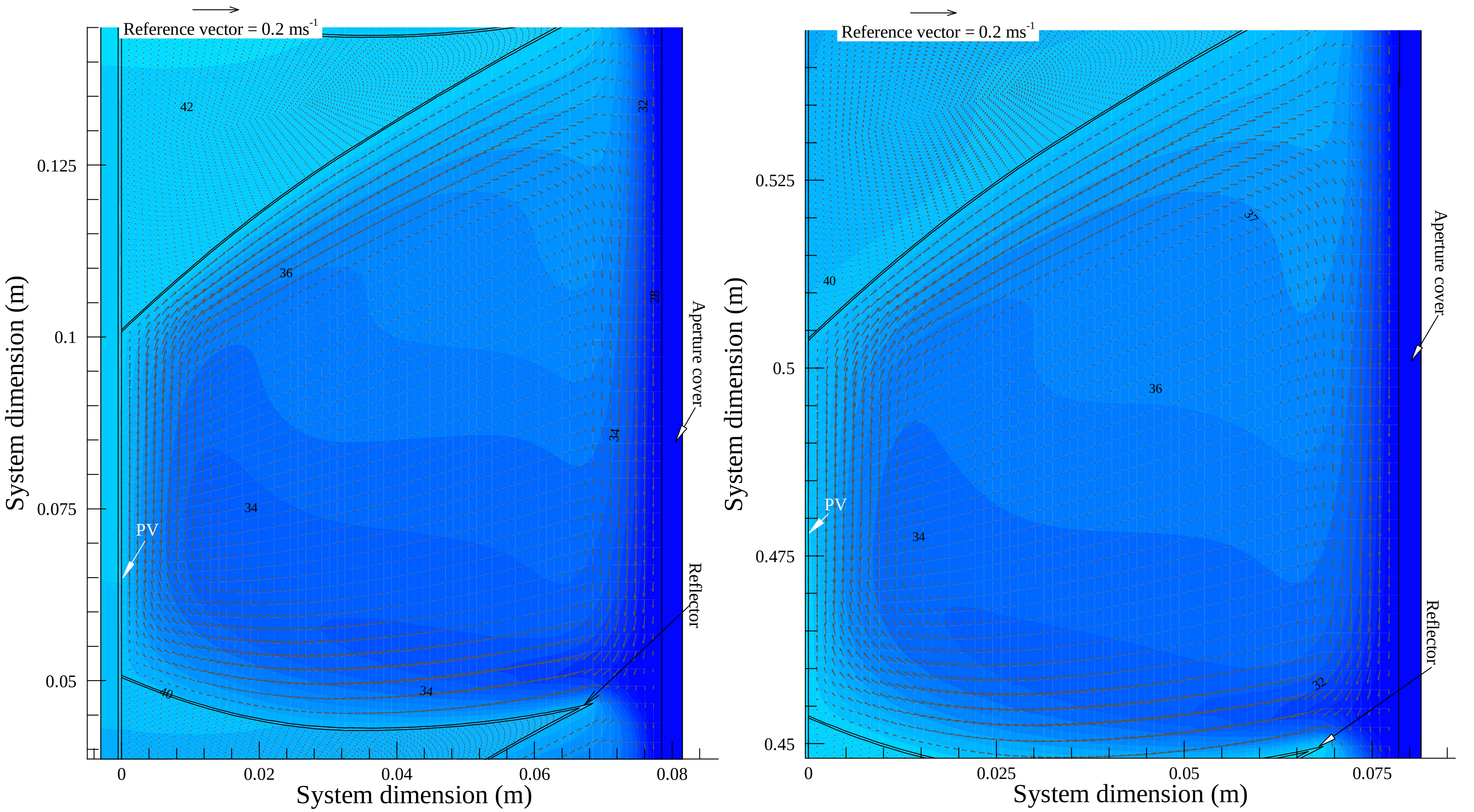


(a)

(b)

Figure 7.3.4 The enlarged view of predicted isotherms and velocity vectors of ACPPVC-50 with heat loss from the aluminium back plate of 23.3 $Wm^{-2}K^{-1}$ inside (a) 1st trough (b) 5th trough. The isotherms are at 1°C intervals. The velocity vector is scaled to a reference vector of magnitude of 0.2 $ms^{-1}$. The solar radiation intensity was 900 $Wm^{-2}$ incident at the aperture cover at an angle of 60°.

## 7.4 Analysis of the Electrical Power Losses for the ACPPVC-50 System

The electrical power loss was due to the resistive loss in the interconnections between solar cells. The solar cells were connected using 0.0004m thick and 0.007m wide tin-lead coated copper strip. In each string solar cells are 52-mm apart leading to a significant power loss. An extra resistance may have occurred because of connection soldering to the solar cells which will increase series resistance '$R_s$' and reduce the maximum power point and thus the electrical conversion efficiency of the PV panel. This was verified by fabricating two different flat PV panels. These systems were

- F1: a string of five solar cells connected in series 52-mm apart
- F2: a string of five solar cells connected in series 2-mm apart.

The fabricated panels are shown in figure 7.4.1. Both systems do not include EVA and front cover glass with a rear aluminium back plate and the same measurements procedure was implemented as detailed in chapter 6. In both systems were measured simultaneously with a complete set of measurements taking less than 10 seconds.


Figure 7.4.1 Non-concentrating solar panels with (a) 52-mm (b) 2-mm tab spacing between individual solar cells without EVA and no glass cover.

### 7.4.1 Experimental Verification of Ohmic Loss For Two Non-Concentrating Flat Panels

The ohmic loss occurred due to the resistance of the inter connecting cable between the individual power sources i.e. if the current in the inter connecting cable is '$i$' and the resistance is $r$ then the power loss will be $i^2r$. The series resistance of a solar cell decreases the maximum achievable output power and comes from the base contact resistance, base bulk resistance, sheet resistance of the emitter layer, metallic resistance of the emitter layer and metallic resistance of the electrodes (Dadu et al., 2002). Figure 7.4.1.1 shows that the variation of maximum power point and percentage of maximum power point difference for the long and short tab non-concentrating flat panel with the incident solar radiation. The experiment was undertaken on the 14th October 2002. The average wind speed was 1.0 $ms^{-1}$ and the ambient temperature was 20 °C. The measurements were taken at 10 second intervals for 6-hours. As expected the maximum power varied linearly with incident solar radiation intensity. The solar panel with 2-mm tab spacing between individual solar cells had higher maximum power compared to the long 52-mm tab spaced solar cells. This is because of the power loss through the interconnections between individual solar cells. The maximum power difference between the ACPPVC-50 system and the non-concentrating flat panel varied from a minimum of 2% at high solar radiation intensities to a maximum of 11% at lower solar radiation intensities, giving an average 5-6% power difference between the systems. The lower maximum power difference at higher solar radiation intensities is due to the temperature of the system and its different components.

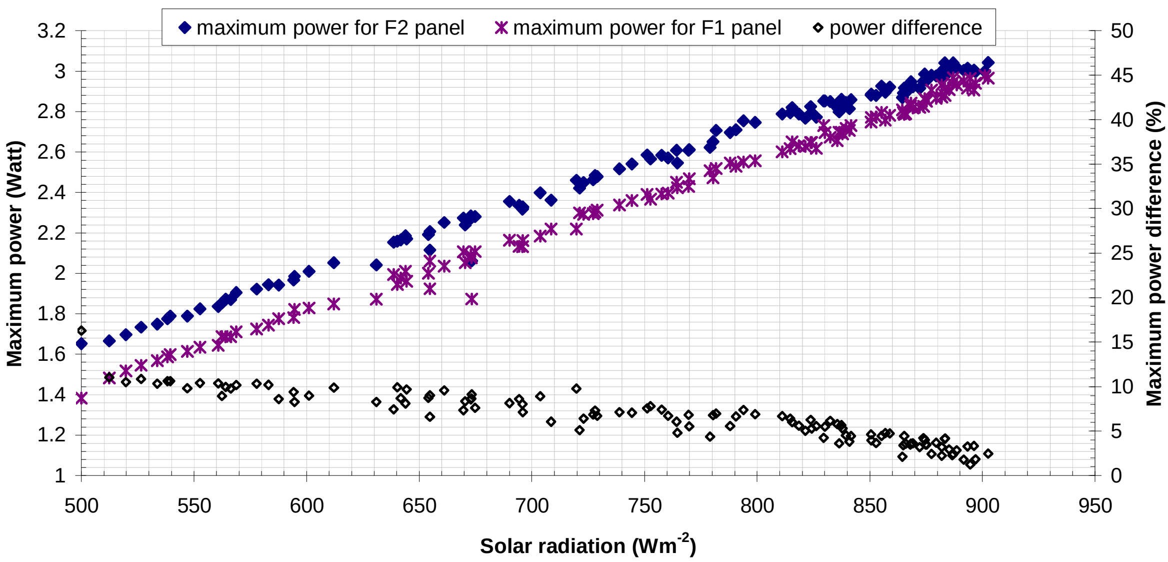


Figure 7.4.1.1 Maximum power point and difference in maximum power point with intensity of incident solar radiation for the long and short tabbed non-concentrating flat solar panel.

Figure 7.4.1.2 shows that the variation in power generated by each PV panel with the voltage developed by it for two solar radiation intensities. There is a significant difference in open circuit voltage between the 52-mm tab spaced solar cells and the 2-mm tab spaced solar cells. This is partially due to the series resistance between the connecting wire and the solar cell for the front and rear connections (Kaminski et al., 1999; El-Advari and Al-Nuaim, 2001; Dadu et al., 2002). Figure 7.4.1.3 shows the electrical conversion efficiency of the long and short tab spaced solar panel with incident solar radiation. The maximum electrical efficiency of the 2-mm tab solar panel is 10.8% compared to an efficiency of 10% for the 52-mm tab spaced solar panel, illustrating the power difference for the long and short tab solar cell panels.

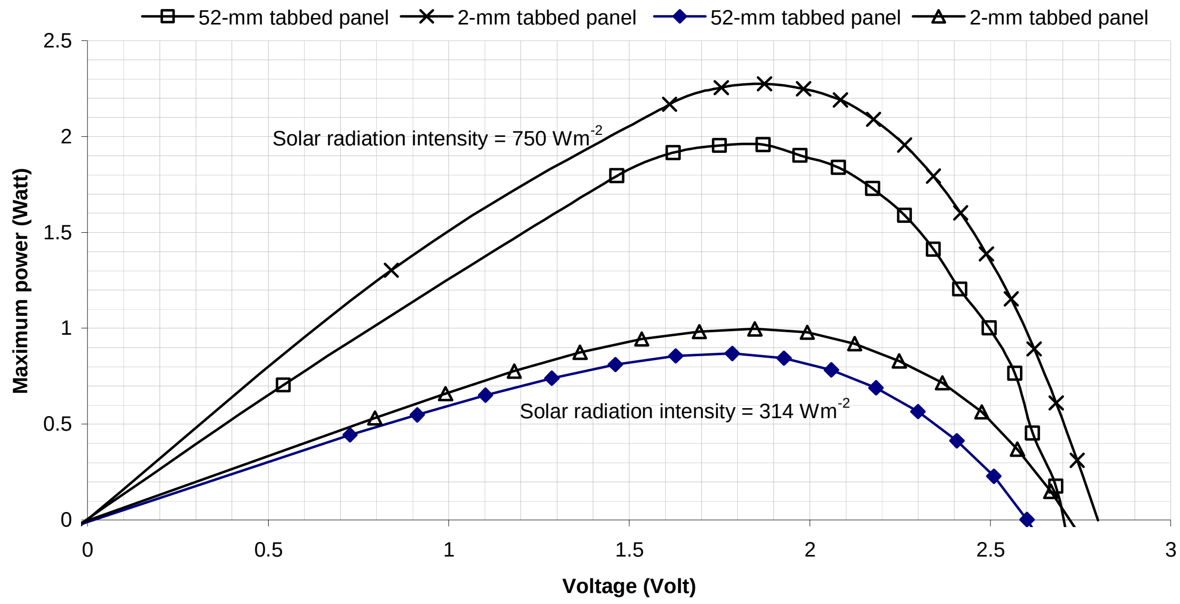


Figure 7.4.1.2 The power developed for the long and short tabbed non-concentrating flat solar panel with the voltage developed by the system for different incident solar radiation intensities.

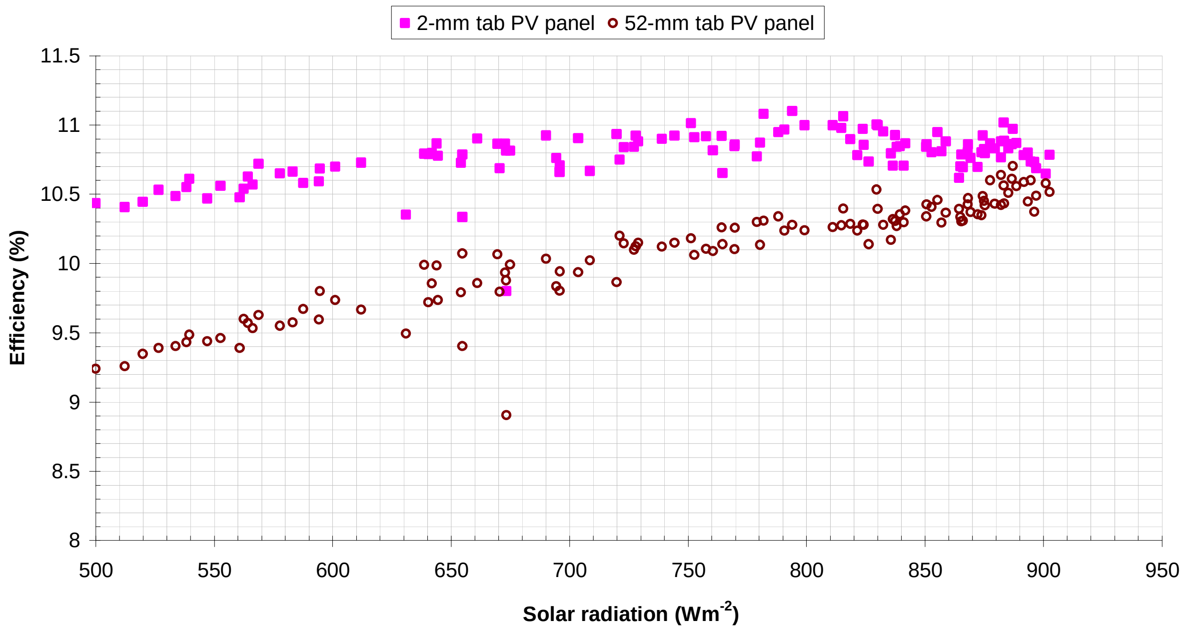


Figure 7.4.1.3 Efficiency for long and short tabbed solar cell panels with incident solar radiation intensity. The average ambient temperature was 20°C.

### *7.4.2* Optical Losses at the Reflector

Power loss occurred due to the optical losses at the reflector and the incidence angle of the solar radiation (Zacharopoulos et al., 2000). The optical analysis presented in chapter 2 for the ACPPVC-50 showed that the maximum optical efficiency achieved by the ACPPVC-50 system was 85.25% i.e. the power loss due to optics is approximately 15% for a wide range of incident angles of solar radiation.

### *7.4.3* Temperature Coefficient and Hot Spot Effect

For every 1°C increase in solar cell temperature the electrical conversion efficiency decreases by 0.5% for single crystal solar cells (Brinkworth et al., 1997). Figure 7.4.3.1 shows the predicted solar cell temperature in the vertical direction for the solar cells when the heat loss coefficient from the rear aluminium plate was 13.7 $Wm^{-2}K^{-1}$ and 23.3 $Wm^{-2}K^{-1}$. The distance was measured from the base of the lowest solar cell to the top of the upper solar cell. The central PV solar cell had the highest predicted temperature resulting in a localised 'hot spot'. This may be explained because of the heat loss from the wooden frame and 'edge effects' on the aluminium back plate. A temperature difference of 3.8°C occurred between the highest and lowest instantaneous temperature of the solar cells. This implies approximately a 2% electrical efficiency decrease for each individual PV string.

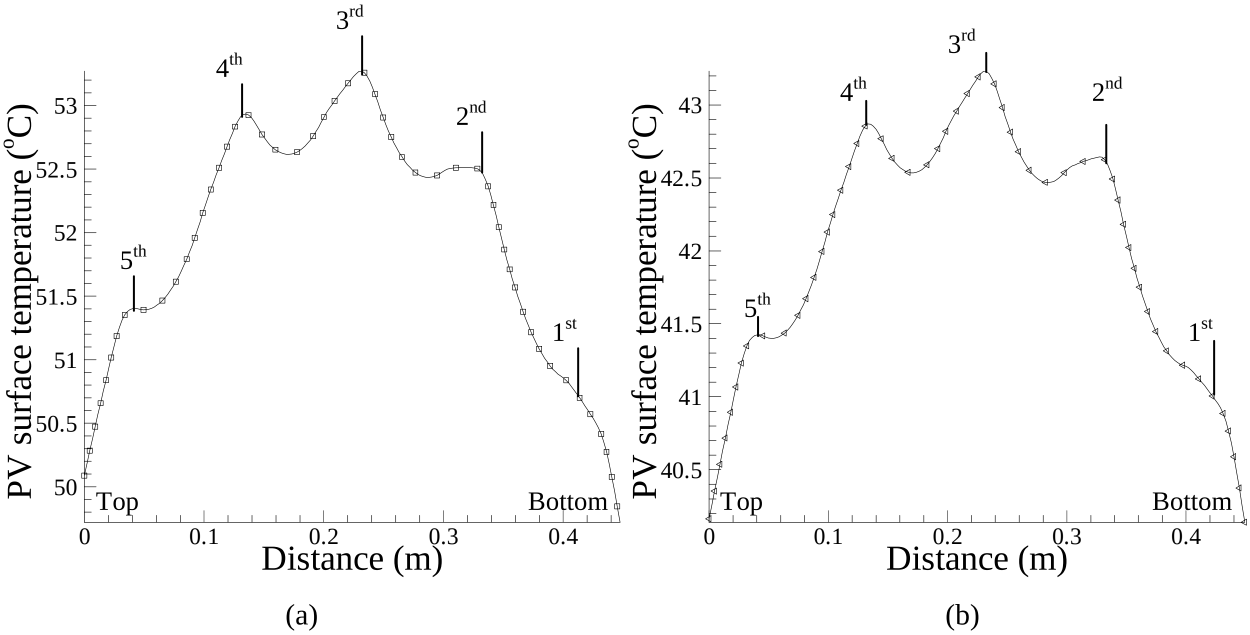


Figure 7.4.3.1 Change in predicted PV surface temperature in the vertical direction for heat loss coefficients of (a) 13.7 $Wm^{-2}K^{-1}$ and (b) 23.3 $Wm^{-2}K^{-1}$ from the aluminium back plate to the ambient. The incident solar radiation was 900 $Wm^{-2}$.

### *7.4.4* Mismatch Loss Between Inter Connected Solar Cells

Mismatch loss occurrs for the photovoltaic panels because of differences in the short circuit current and open circuit voltage between individual solar cells (Ho and Wenham, 2001). From a sample of ten solar cells (BP Saturn, Anon, 2001e), the open circuit voltage differed by 0.5% and short circuit current by 3.5% (Eager et al., 2002). The implication of varied solar cell performance can result in a power difference of up to 5% in the ACPPVC-50 system. Although mismatch occurs for both the non-concentrating flat system and ACPPVC-50 system, the mismatch power loss for the ACPPVC-50 system is 2 to 3% higher because of the increased solar radiation level due to concentration, variations in solar cell temperature and non-uniform illumination of the cells.

## *7.5* Model Validation

The finite element model has been verified using the temperature measurements at different position of the rear aluminium back plate and at the reflector substrate. The solar radiation considered for the model was 900 $Wm^{-2}$ incident at an angle of 60° to the aperture cover. The experimental investigation took several days, the clearest day (23rd September 2002, see page 218) was used for validation of the finite element model (all experimental result are shown in section 6.4.7). It is observed from figure 6.4.7.3 (see page 218) that both systems were exposed for more than three and half hours with incident solar radiation intensity greater than 800 $Wm^{-2}$ and one an hour more than 900 $Wm^{-2}$, therefore the solar radiation intensity of 900 $Wm^{-2}$ was used to validate the finite element model.

### *7.5.1* Predicted and Experimentally Measured Temperatures

Good agreement of the temperatures of the rear aluminium back plate, reflector substrate and temperature of the inside aperture cover glass were obtained between the experiment and simulations. Table 7.5.1 shows the experimentally measured and simulated temperatures at different thermocouple locations. The thermocouples were located as shown in figure 6.3.3 and figure 6.3.4 in chapter 6. The ACPPVC-50 system was exposed for nearly 68 minutes with a solar radiation of greater than 900 $Wm^{-2}$, with the highest peak of 987 $Wm^{-2}$, therefore a peak of 10% variation in solar radiation occurred in the experimental results. The measured ambient temperature was 20°C±1°C (approximately 14:00 in figure 6.4.7.2, page 218). For the simulation the temperatures were extracted from the isotherm plots shown in figure 7.3.1(b). It is considered the system temperatures achieved are close to steady state conditions with an average solar radiation of 900 $Wm^{-2}$. The temperature between the experiments and simulation lies within ±6%. Good agreement occurs between experiments and simulations.

| | | Thermocouple location | Experimental temperature ($T_e$ °C) | Simulated temperature for heat loss coefficient of | | | Temperature difference[1] |
|---|---|---|---|---|---|---|---|
| | | | | 3.7 Wm$^{-2}$K$^{-1}$ ($T_{max}$°C) | 13.5 Wm$^{-2}$K$^{-1}$ ($T_s$°C) | 23.3 Wm$^{-2}$K$^{-1}$ ($T_{min}$°C) | $\frac{(T_e - T_s)}{T_e} \times 100$ % |
| Materials | Aperture cover glass | Tgi36 | 34.5 | 41.2 | 32.5 | 25.3 | -5.8 |
| | | Tgi37 | 35.6 | 46.0 | 34.9 | 26.2 | -1.9 |
| | Reflector substrate | Tr38 | 50.7 | 93.0 | 48.7 | 39.6 | -3.9 |
| | | Tr39 | 49.3 | 97.0 | 50.6 | 41.3 | +2.6 |
| | | Tr40 | 54.4 | 100.0 | 52.3 | 42.4 | -3.8 |
| | | Tr41 | 52.6 | 101.3 | 52.4 | 42.7 | -0.38 |
| | | Tr42 | 52.5 | 101.0 | 51.1 | 41.2 | -2.6 |
| | | Tr43 | 48.6 | 100.7 | 49.8 | 40.2 | +2.5 |
| | Aluminium substrate | T60 | 49.4 | 99.4 | 50.5 | 40.9 | +2.2 |
| | | T61 | 51.2 | 104.3 | 53.2 | 43.2 | +3.9 |
| | | T62 | 49.3 | 103.2 | 50.9 | 40.8 | +3.2 |

Table 7.5.1 Experimentally measured and simulated temperatures for the ACPPVC-50 at different locations. The incident solar radiation for the simulation was 900 Wm$^{-2}$ and the experiment was conducted on the 23rd of September 2002.

[1] Temperature difference is based on a simulated temperature for heat loss coefficient of 13.5 Wm$^{-2}$K$^{-1}$.

### 7.5.2 I-V Curves For Experiment and Simulation

The second method used to validate the model is using the I-V curve for the ACPPVC-50 panel with different solar radiation intensities. Figure 7.5.2.1 shows the comparison between simulated and experimental I-V curves for 700 and 900 $Wm^{-2}$ incident solar radiation. The average predicted solar cell temperature was 45°C when the incident solar radiation was 900 $Wm^{-2}$ and 33°C when the incident solar radiations 700 $Wm^{-2}$. The temperature simulated at each element in the finite element model was directly incorporated into the electrical model detailed in Appendix A (page 267). Excellent agreement was observed for the I-V curves. The maximum power point varies by 1.5% for incident solar radiation of 900 $Wm^{-2}$ whereas the maximum power point changes by less than 0.6% when the incident solar radiation was 700 $Wm^{-2}$.

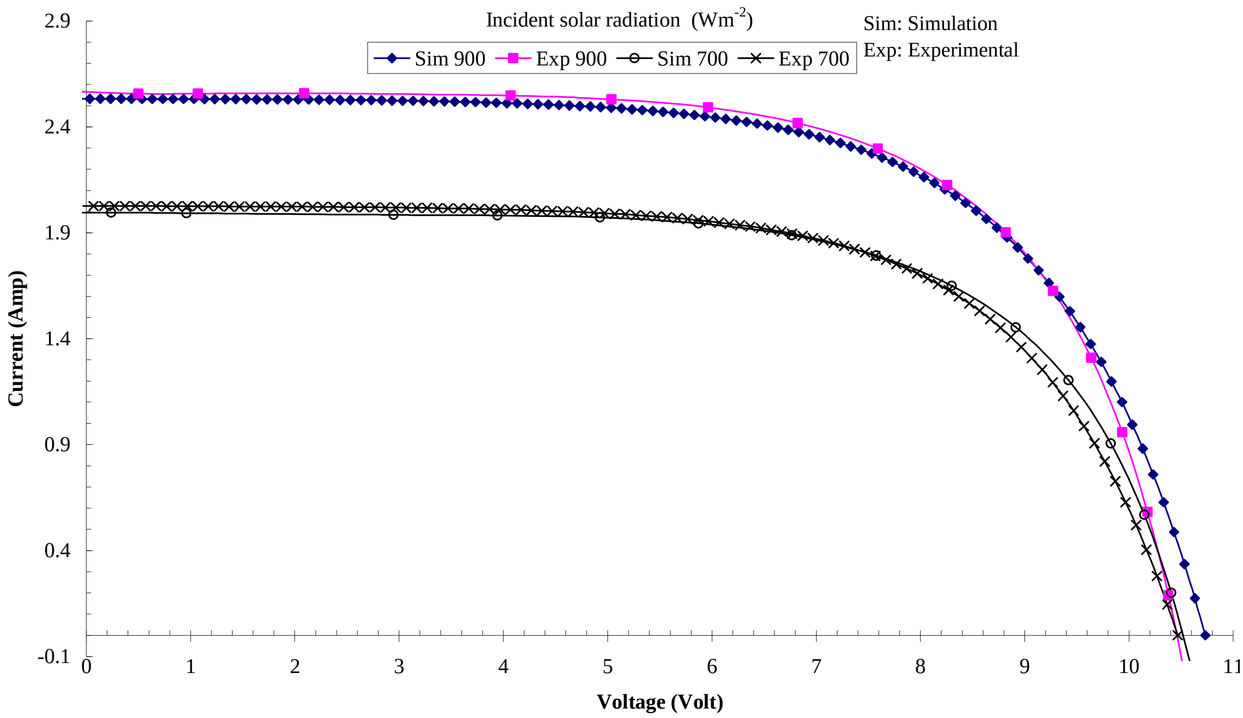


Figure 7.5.2.1 Predicted and measured I-V curves for different solar radiation intensities.

## 7.6 Conclusions

The choice of boundary conditions and the heat loss coefficients is important for predicting the heat transfer within an asymmetric compound parabolic photovoltaic concentrator. Depending on the average wind velocity at the rear of the aluminium back plate, by determining the Reynolds and Nusselt number, the most probable heat loss coefficient is considered to be approximately 13.7 $Wm^{-2}K^{-1}$. The parametric analysis of heat transfer within the ACPPVC-50 for different heat loss coefficients at the rear of the aluminium back plate shows that the maximum solar cell temperature of 99°C may occur at very low wind speeds i.e. a heat loss coefficient of 3.7 $Wm^{-2}K^{-1}$, whereas the solar cell surface temperature decreases to 41°C at high wind speeds of $5ms^{-1}$ i.e. a heat loss coefficient of 23.3 $Wm^{-2}$ $K^{-1}$. The comparative performance analysis of long and short tabbed solar strings shows that an average 5 to 6% electric power loss occurred due to the ohmic loss in the interconnections between each individual solar cell for the ACPPVC-50 system and partially explains the power ratio of 1.5 to 1.62 even though the ideal concentration ratio is 2.0. Predicted optical analysis showed that an optical loss of up to 15% can occur in the ACPPVC-50. An additional 1 to 2% optical loss may occur due to the creation of gaps between the solar cells and reflectors.

The modified 'comprehensive unified' model has been validated using the following two methods:

- Temperature measurements: Predicted and measured temperatures at the aluminium back plate, at the reflector substrate and at the inside covers glass were compared.
- I-V curve measurement: The temperatures determined at each system component from the 'finite element' model were directly incorporated into the electrical model and used to predict the I-V curve of the 'PV' system which were then compared with experimental measurements.

Both validation methods gave a good agreement between the experiment and predictions, and the temperature difference at different points was less than ±6%, whereas the maximum power point differs by less than 1.2%.